AN EXPERIMENTAL AND KINETIC MODELING STUDY OF GLYCEROL PYROLYSIS

F. Fantozzi[a], A. Frassoldati[b], P. Bartocci[a], G.Cinti[a], F. Quagliarini[c], G. Bidini[a], E.M. Ranzi[b]

[a] Department of Engineering, University of Perugia, Via G. Duranti 67, 06125 Perugia, Italy

[b] Politecnico di Milano, Dipartimento di Chimica, Materiali e Ingegneria Chimica, Giulio Natta, Piazza Leonardo da Vinci 32Milano, Italy

[c] FAIST Components Spa, Via dell'Industria, 2 06014 Montone (Perugia), Italy

*Corresponding author: bartocci@crbnet.it

Abstract

Pyrolysis of glycerol, a by-product of the biodiesel industry, is an important potential source of hydrogen. The obtained high calorific value gas can be used either as a fuel for combined heat and power (CHP) generation or as a transportation fuel (that is hydrogen to be used in fuel cells). Optimal process conditions can improve glycerol pyrolysis by increasing gas yield and hydrogen concentration. A detailed kinetic mechanism of glycerol pyrolysis, which involves 137 species and more than 4500 reactions, is drastically simplified and reduced to a new skeletal kinetic scheme of 44 species involved in 452 reactions. An experimental campaign with a batch pyrolysis reactor was properly designed to further validate the original and the skeletal mechanisms. Comparisons between model predictions and experimental data strongly suggest the presence of a catalytic process promoting steam reforming of methane. High pyrolysis temperatures (750-800°C) improve process performances and non-condensable gas yields of 70%w are achieved. Hydrogen mole fraction in pyrolysis gas is about 44-48%v. The skeletal mechanism developed can be easily used in Computational Fluid Dynamic software, reducing the simulation time.

Keywords: Glycerol; Pyrolysis; Skeletal model; Syngas; Hydrogen; Biofuels.

1. Introduction

EU goals for biofuels, as set out in the RED 2009/28/EC (see mandatory goals) [1], have promoted the use and production of biodiesel. The EU Energy and Climate Change Package (CCP) became operative on April 6, 2009. The Renewable Energy Directive (RED), which is part of this package, came into effect on June 25, 2009. The CCP includes the "20/20/20" goals for 2020: a reduction of 20% in greenhouse gas (GHG) emissions compared to 1990; an improvement of 20% in energy efficiency (compared to forecasts for 2020) and a 20% share of renewable energy in the total European energy mix. Part of this last 20% share is represented by a 10% minimum target for biofuels in the transport sector to be achieved by all Member States. This percentage was slightly modified by a proposal of Indirect Land Use Change (ILUC). Given this framework, the current biofuels scenario will bring to a stable production of first generation biofuels, that will hardly

increase, and a slight increase in second generation biofuels (second generation bioethanol mainly). New European targets should be still fixed.

The 2014 USDA Foreign Agriculture Service statistics [2], show that a production of biodiesel equal to 10,890 Ml was reached in Europe in 2014, this means a production of 916,000 t per year of glycerol. This product has an interesting energy content and can be used to provide heat and electricity to the same transesterification plant, as it is reported in D'Alessandro et al. 2011 [3]. The analyses proposed by Fantozzi et al. 2014 [4], Manos et al. 2014a [5] and Manos et al. 2014b [6] describe how integrating CHP technologies inside a biofuel plant is part of the "agroenergy district" promotion strategy. Authayanun et al. 2013 [7] have performed experiments feeding directly glycerol in a high-temperature polymer electrolyte membrane fuel cell (HT-PEMFC). Beatrice et al. 2014 [8] have tested in a compression engine a bio-derivable glycerol-based ethers mixture (GEM). Besides Beatrice et al. 2013 [9] have also synthesized an oxygenated fuel additive (glycerol alkyl-ether) suitable for blending with diesel and biodiesel. Martín and Grossmann 2014 [10] have performed fermentation tests on glycerol. Nanda et al. 2014 [11] have designed and tested a continuous-flow reactor for the conversion of glycerol to solketal, through ketalization with acetone. Pedersen et al. 2016 [12] have performed hydrothermal co-liquefaction of aspen wood and glycerol with water phase recirculation.

Pyrolysis of glycerol and reforming are interesting techniques that have been already used to produce hydrogen to be used for transportation, see Wulf et al. 2013 [13].

Several works in literature take into account pyrolysis or gasification of glycerol. Experimental works can be classified based on reactor typology and process parameters.

Encinar et al. 2010 [14] used cylindrical tube of stainless steel 316, set in vertical position. In the upper part of the reactor a thermocouple was used to control the temperature. A second reactor was placed under the first one, with the aim to increase the residence time of the material at reaction temperature. Solution of water and glycerol is inserted inside the reactor with the help of a pump.

In the work of Fernandez et al. 2009 [15] pyrolysis of glycerol was performed in an electrically heated furnace and in a microwave reactor. Glycerol was supplied to the upper part of the reactor through an injector, and activated charcoal was used as a catalyst for the reaction.

Peres et al. 2010 [16] have performed continuous pyrolysis tests in a steel reactor that was filled with alumina oxide. A pump used for liquid gas chromatography was employed to supply glycerol in the reactor. The reactor was heated using an electrical furnace. Gas produced were sampled in tedlar bags. Vallyiappan 2004 [17] and Vallyiappan et al. 2008 [18] used a packed fixed bed reactor full of quartz and silicon carbide, which were used to simulate a plug flow reactor. Packing material was contained inside a plug of quartz wool, which was inserted on a supporting mesh at the center of reactor. Vallyiappan obtained interesting yields of hydrogen (about 50% in volume), performing pyrolysis at 800°C. Baker-Hemings et al. 2012 used these sets of experimental data [19] to develop and validate a detailed kinetic model of glycerol pyrolysis.

A detailed CFD model of the above hinted reactors has never been reported in literature, for this reason this work has two main goals. One is to provide new experimental data, aimed at further validating a detailed kinetic mechanism for glycerol pyrolysis. The second goal is to develop a simplified skeletal kinetic mechanism, suitable for CFD simulations. This new and simplified skeletal mechanism, which represents a novelty in the state of the art of glycerol pyrolysis

simulation, is the added value of this work and it is available in the supplementary material. The new tool can be used in reactor design and optimization.

The paper presents the analysis and optimization of an energy process (pyrolysis of glycerol), to compare its performance with other alternative processes (such as steam reforming or steam gasification), this indicates that the results presented are interesting for the scientific and technical community involved in the development of processes to produce hydrogen from glycerol and to use it in different cogeneration devices (among them fuel cells).

The originality of the work is based on a new skeletal model. This has the advantages to be enough simplified to be used in CFD modeling for reactor optimization. It is the first step in the development of a new process in which a unique reactor can reform glycerol using biochar as a catalyst and achieve an increase of biochar porosity (so partially activating it).

2. Materials and Methods

All the analyses of the samples were performed at the Biomass Research Centre of the University of Perugia, see the analysis protocols described in Bidini et al. 2015 [20]. The proximate analysis of the raw materials and of the char and tar were determined using the thermogravimetric analyzer Leco TGA-701 according to the CEN/TS 14774-14775 [21,22]. The amounts of the principal chemical elements like nitrogen, hydrogen and carbon were characterized by the Leco TruSpec CHN analyzer, according to the UNI EN 15104:2011 [23]. The calorific value of the sample and products was determined with an LECO AC-350 analyzer, according to the UNI EN 14918:2009 [24].

Pyrolysis gas composition was determined by Micro-GC 490, Varian, using a Thermal Conductivity Detector (TCD). The Micro GC includes a heated injector, backflush and Genie membrane filter to remove particles and liquids from analyzed gas samples. The Micro-GC contains two analytical modules: Molecular Sieve capillary column with Argon as carrier gas used for the analysis of CH_4, CO, H_2, O_2, N_2 and Pora Plot Q capillary column with Helium for the analysis of CO_2, C_1-C_3 gaseous species.

A batch reactor used in the laboratory of CRB was employed to perform pyrolysis (see Figure 1). This was already described in Bartocci et al. 2102 [25], Paethanom et al. 2013 [26] and Bidini et al. 2015 [20]. It is a plant in which it was possible to perform pyrolysis of solid/liquid samples and to characterize the products from different experiments. The experimental setup used in the laboratory during this study is shown in previous works, see Bidini et al. [20]. Pyrolysis tests were carried out in a reactor with a height of 30 cm and the inner diameter of 15cm. At the top of the reactor there is a nitrogen inlet pipe (N_2), a valve to feed the glycerol, one thermocouple connected to the P.I.D device to maintain the programmed temperature inside the reactor (T1), one thermocouple to measure the temperature inside the reactor (T2), a pressure sensor (p). The heating system is made of two semi-spherical electric heaters, each with a power of 4.8 kW.

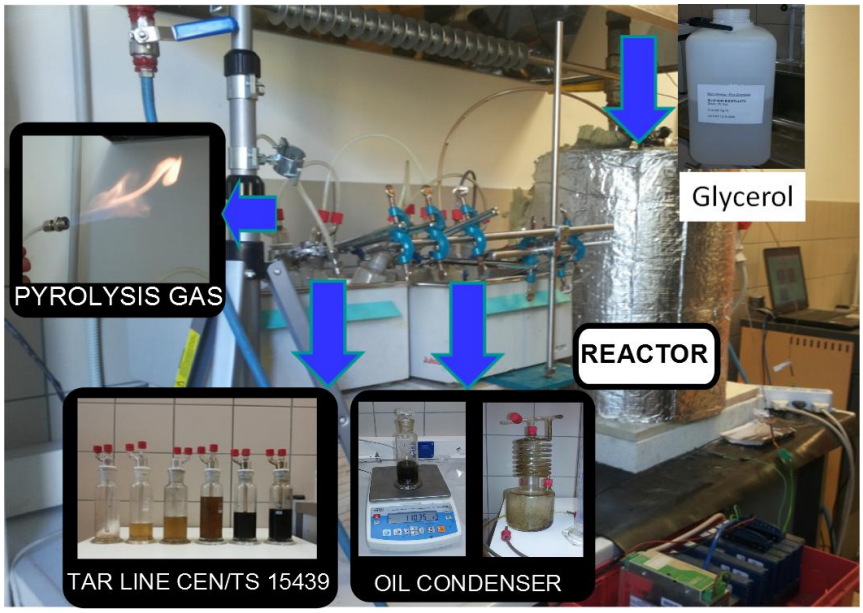

Figure 1: Batch reactor description and tar sampling methodology

Before the experimental test, nitrogen was fed into the reactor to remove air and create inert atmosphere conditions for the pyrolysis process. The reactor was heated from ambient temperature to 600°C at a heating rate of about 20°C/min. When the reactor reached the desired temperature, the sample (of a total mass of 100 g) was gradually inserted into the reactor, with an average mass flow of 3 g/min. Volatiles exited from a pipe and passed through the tar sampling line. The gas sampling line cooled the volatiles temperature, which reached ambient temperature values. The portion of the non-condensable gas was sampled in Tedlar bags and analyzed in a Micro-GC 490. After 30 min the pyrolysis process was completed.

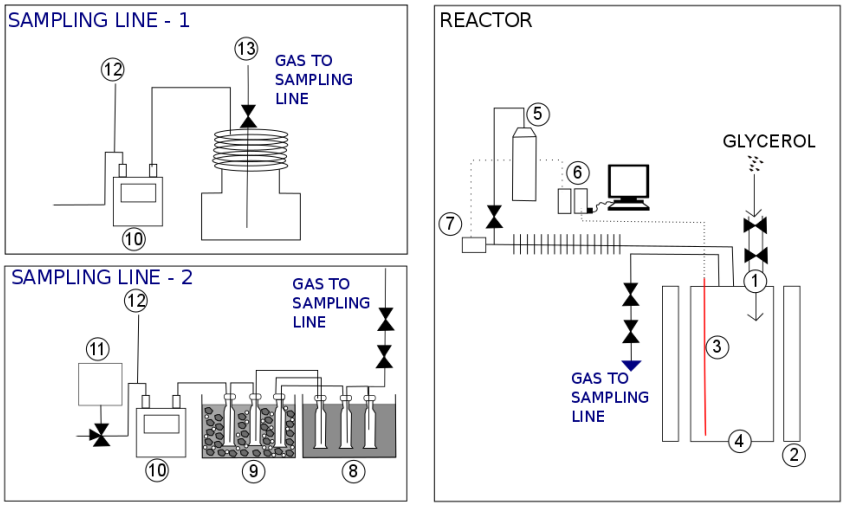

Figure 2: Gas sampling procedures (left) and batch pyrolysis plant layout (right)

Figure 2 reports the layout of the batch pyrolysis plant, where it is shown the DAQ (Data Acquisition) system and the position of the thermocouple used. On the left, two different sampling lines are shown: one (sampling line number 1) with a condenser, which is not filled with a solvent and separates condensable gases based on temperature decrease, another (sampling line number 2) to condense the gases in isopropanol, through adsorption and cooling. The first one was used to sample pyrogas in tedlar bags and then to measure its composition (without having traces of tars in the bags, which could harm the micro-GC). The second one was used to measure mass balance, because when the condensable gases are absorbed in isopropanol it is difficult to separate them (in fact condensed compounds have the same temperature of evaporation of isopropanol). This means that two kinds of tests were performed: one to measure the gas composition and one to measure condensable gases and non-condensable gases masses.

In both the sampling lines presented in figure 2, there is no extraction pump for pyrogas, but it flows through the sampling line, due to the internal pressure of the reactor. The average charge in the reactor was about 36 mg each 22 seconds.

Concluding, it should be stressed that the experimental conditions of the reactor were quite close to ideal conditions, for the following reasons: the mass of the reactor is greater respect to the mass of the raw material which is fed into it; the reactor has been already heated up and has reached a steady temperature; time of reaction is very short. Another aspect which has to be taken into account is the fact that in this case a liquid biomass is used, which vaporizes in a very short period and so undergoes to pyrolysis reaction also very quickly. All these facts make an assumption of a Perfectly Stirred Reactor (PSR) reasonable. This is also a great advantage of glycerol, respect to solid biofuels.

The fact that the working conditions were quite close to ideal conditions implies that kinetics is predominant on heat transfer effect. This was an advantage in the experimental campaign. It was noticed also that the fast heating rates and the high temperatures avoid polymerization and char formation. Small quantities of char, were formed at low temperatures, but they couldn't be weighed, so it was assumed that these were not significant.

The internal heating rate can be calculated based on the average retention time of about 22 seconds. this implies heating rates of about 17°C/s, 22°C/s, 26°C/s, 28°C/s and 31°C/s, respectively for temperatures of 400°C, 500°C, 600°C, 650°C and 700°C (considering an ambient temperature of 20°C). A fully batch test was made at the beginning of the experimental campaign. With an average heating rate, typical of the batch reactor (i.e. 20°C/min), the result was to have glycerol evaporation, instead of its pyrolysis. For this reason, it was chosen to heat up the reactor and then to insert glycerol in an already heated environment. In this case, the reactor can be used in a continuous way and can be directly coupled to an internal combustion engine or a fuel cell. This is another advantage of glycerol pyrolysis if compared with biomass pyrolysis.

Char yield (CY) is expressed as the weight ratio between the solid residue (SR) and the raw material (RM). Gas yield (GY), always referred to the raw material, was measured by the flowmeter and converted in mass knowing the gas composition and its exit temperature. Finally, Tar Yield

(TY) is simply obtained by difference. Control tests were performed to check data obtained, using a condenser to control the results on tar.

In literature there are different methods for tar sampling, some have been presented by Paethanom et al. 2013 [26], Phuphuakrat et al. 2010 [27] and Michailos et al. 2012 [28]. In this study, the sampling line was designed on the basis of CEN/TS 15439:2006 [29]. Volatiles produced by pyrolysis passed through a series of six impinger bottles where tar is collected by condensation and absorption. The last bottle is empty. The total volume of isopropyl alcohol used as sampling solvent in the first five bottles is 500 ml (100 ml on the each bottle). The series of impinger bottles was placed in two separate baths. Bottles 1, 2 and 3 are placed in an electrically heated water bath at +35°C, while bottles 4, 5 and 6 are cooled with NaCl/ice eutectic mixture in a proportion of 3:1 to obtain -20±1°C. It took about 15 min to reach final temperature. The sampling train was connected with a gas flow meter. After the test all the content of impinger bottles was gathered in a unique flask and evaporated with a rotary evaporator, to separate the solvent from tar in accordance with CEN/TS 15439:2006 [29]. The residue in the flask was weighed to determine the quantity of gravimetric tar. Tar or biooil produced from glycerol pyrolysis was measured both using the above mentioned tar line and a condenser. The advantage of using the condenser was to avoid tar mixing with isopropanol. Figure 3 shows pyrolysis products characterization methodology.

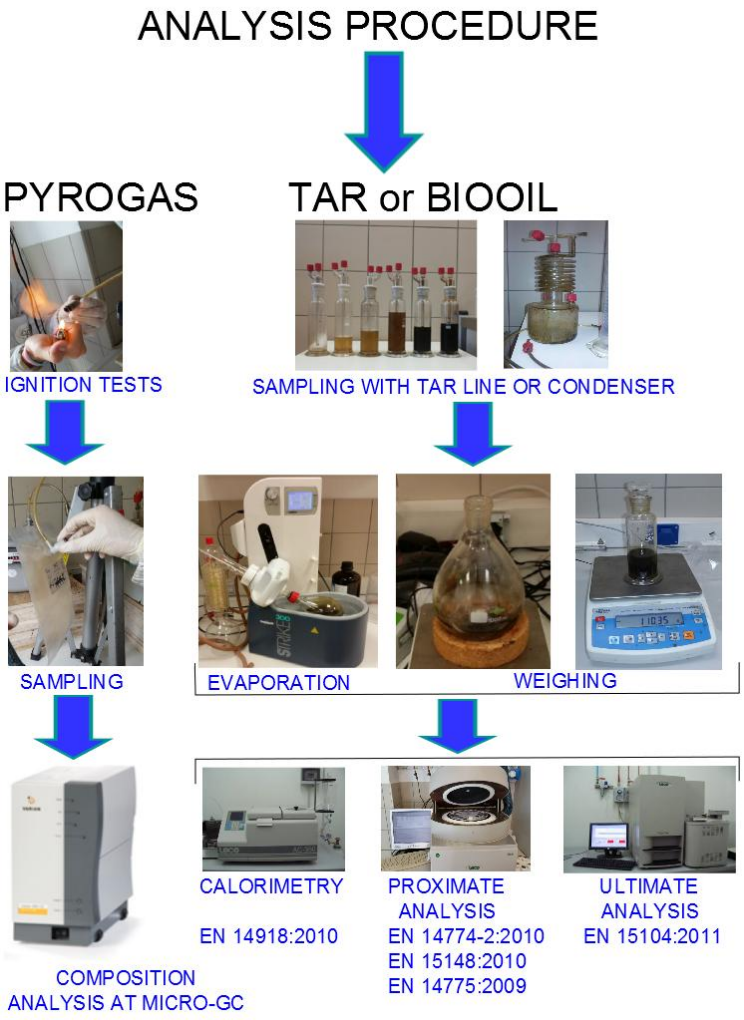

Figure 3: Pyrolysis products characterization methodology

As already mentioned, pyrogas is collected in tedlar bags and analyzed with a micro-GC 490, Varian. Tar is sampled both using a tar line and a condenser. In a first test, the tar line is used to absorb all the tar and avoid it going in the tedlar bags, in this way the microGC is protected. In a second test, it was used a condenser to collect all the tar in purity, without mixing it with the isopropanol contained in the tar line. Then tar was characterized using a thermogravimetric balance to perform proximate analysis an LECO Truespec CHN analyser and a bomb calorimeter. No important quantities of char were found inside the reactor after the tests. All tests were performed in triplicate.

3 Experiments: glycerol pyrolysis in a batch reactor

3.1 Glycerol characterization and pyrolysis experimental tests

The results of pure glycerol characterization analysis (see Table 1) show that it has a slightly higher LHV, compared to biomass and a similar concentration of carbon, hydrogen, and oxygen. Hydrogen content is also a little higher.

Table 1: Glycerol characterization

	Pure glycerol	Standard deviation
Moisture [%w]	0	0.3
Ash [%w]	0	0.2
Volatiles [%w]	100	0.5
Fixed Carbon [%w]	0	0.1
HHV [kJ/kg]	19,000	515
Carbon [%w]	39.13	0.3
Hydrogen [%w]	8.70	0.1
Nitrogen [%w]	-	0.05
Oxygen [%w]	52.17	0.3

The results of pyrolysis tests are shown in Table 2. It can be seen that increasing temperature non-condensable gas yield increases, especially for temperatures higher than 500°C. Table 2 also shows the composition of non-condensable gases, always as a function of the pyrolysis temperature. Hydrogen concentration increases with the increase of temperature, carbon monoxide, and carbon dioxide concentrations decrease, while methane has a nearly constant behavior. Ethylene concentration decreases also with the increase of temperature.

Table 2. Yields of condensable and non-condensable gases and molar gas compositions.

	400°C		500°C		600°C		650°C		700°C	
	Yields	Standard Deviation	Yields	Standard Deviation	Yields	Standard Deviation	Yields	Standard Deviation	Yields	Standard Deviation
Non condensable gas yields [%w]	**19**	1.1	**51**	1.5	**60**	1.3	**63**	1.4	**67**	2
Condensable gas yields [%w]	**81**	1.8	**49**	1.6	**40**	2.1	**37**	1.2	**33**	1.1
				Molar gas composition [%v]						
		Standard Deviation		Standard Deviation		Standard Deviation		Standard Deviation		Standard Deviation
H_2	**15**	2.1	**18**	2.3	**25**	2.1	**30**	2.7	**35**	2.5
CO	**45**	2.8	**45**	2.5	**42**	2.3	**40**	1.9	**39**	2.3
CO_2	**10**	1.1	**7**	0.9	**3**	0.5	**3**	0.2	**2**	0.1
CH_4	**12**	3.2	**14**	3.1	**16**	2.8	**15**	2.5	**15**	2.1
C_2H_4	**18**	2.5	**16**	2.3	**14**	2.1	**12**	1.5	**9**	1.2
TOT	**100**	-	**100**	-	**100**	-	**100**		**100**	

In Figure 4 a bar chart reporting mass yields of non-condensable and condensable gases is shown, being the production of a solid fraction negligible, the mass balance is closed by the two gaseous components.

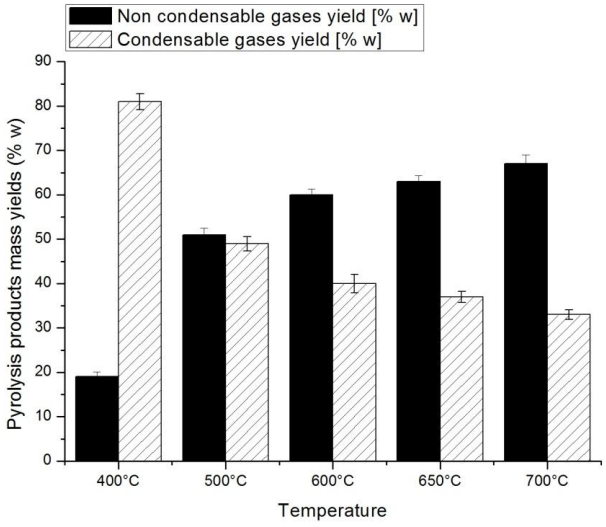

Figure 4: Bar chart reporting pyrolysis products yields

The standard deviation of gas composition and gas yields values is due to the difficulty of the experimental apparatus to regulate precisely the mass flow of glycerol inside pyrolysis reactor; this implies a slight variation in residence time inside the same. Residence time obviously influences the gas composition and reaction kinetics.

4 Kinetic Scheme and Numerical Methods

4.1 Numerical Methods

The software DSMOKE, developed by the CRECK modeling group of the Politecnico di Milano, was used for the simulation reported in this work. It is an easy platform to launch a simulation using detailed kinetic schemes developed and available online in [30]. An isothermal PSR reactor was assumed and simulations were performed at different temperatures between 823 K and 1073 K. Once reaction temperature was fixed, the effective residence time of reactants inside the reactor volume (5 liters) was evaluated accounting for the mass flow of glycerol inserted into the reactor (3 g/min) and an effective and average density of reacting mixture. Thus, the residence time inside the reactor was ~130 ms at 923 K and only ~50 ms at 973 K, mainly due to the different glycerol conversion.

4.2 Glycerol pyrolysis modeling

The major radical reaction steps in the pyrolysis of glycerol are the initiation and the H-abstraction reactions, which refer to the different types of hydrogen atoms available in the glycerol molecule. As already discussed by Barker-Hemings et al. 2012 [19], molecular dehydrations are interesting reaction pathways as well. Figure 5 summarizes both these radical and molecular reaction paths. The primary propagation reactions of glycerol, coupled with a general kinetic scheme of hydrocarbon pyrolysis and oxidation (Ranzi et al., 2012 [30]), were also tested against several sets of experimental data, offering good agreement between predicted and measured values.

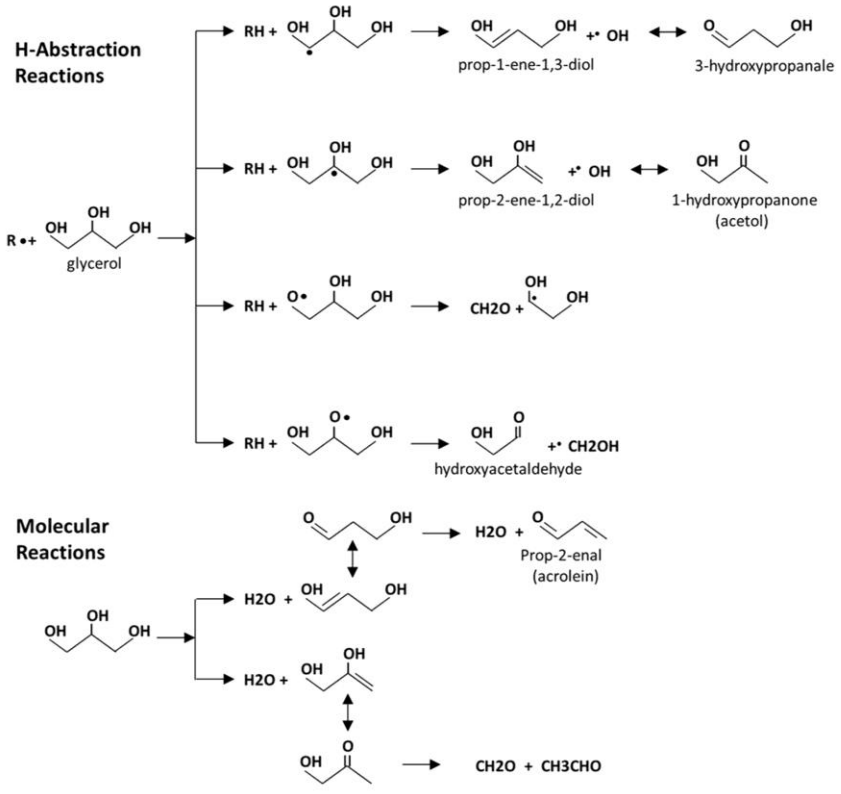

Figure 5: Primary reactions of glycerol pyrolysis

Figure 6 shows the concentration profiles of the major species involved in the reaction system. Acetol and 3-hydroxypropanal are very reactive intermediates rapidly decomposing to form the most stable species, such as acetaldehyde and acrolein. Successive pyrolysis of these species further contributes to syngas formation. CO and H_2 profiles clearly indicate that they are only successive decomposition products.

The overall kinetic scheme POLIMI_BIO1407, already validated by Barker-Hemings et al. 2012 [19], used in these simulations is constituted by 137 species and 4500 reactions and it is not adequate for CFD simulations. For this reason, it is necessary to develop a reduced mechanism that can be used for this purpose.

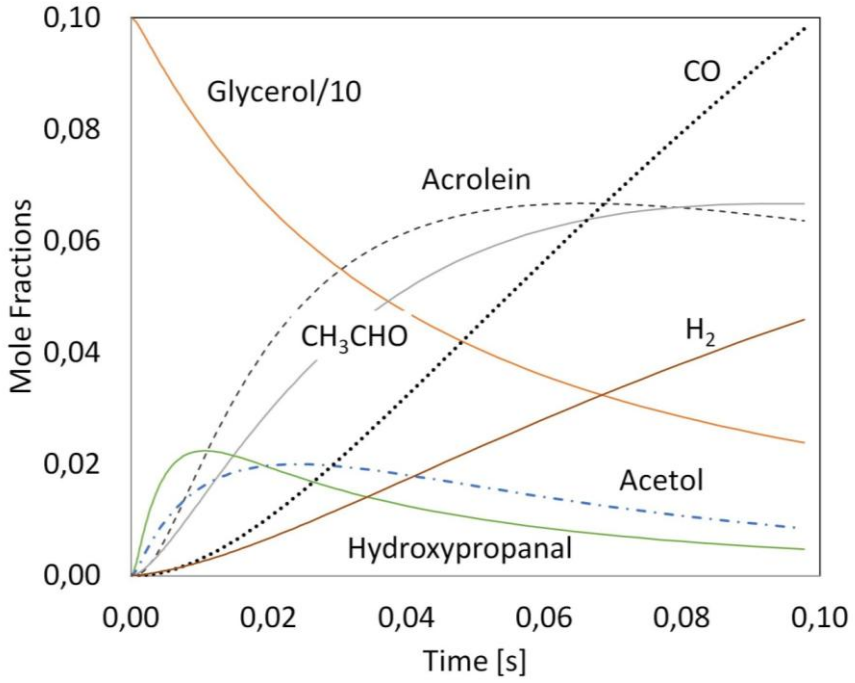

Figure 6: Primary and successive reaction products of glycerol pyrolysis at 700 °C and 1 atm (model predictions)

4.3 Development of a skeletal scheme of Glycerol Pyrolysis

The skeletal kinetic scheme of glycerol pyrolysis has been obtained with the RFA (Reacting Flux Analysis), successively complemented with a sensitivity analysis by Stagni et al., 2014 [31]. The RFA reduction technique analyses the behavior of the original mechanism in ideal reactors. The importance of each species is evaluated according to the production and consumption rates throughout the whole reactor. The total fluxes of each reactor are then normalized with respect to the local maximum value, and according to the required size and precision of the reduced mechanism, only the first *n* species are kept in the skeletal model. The reduced kinetic scheme of glycerol pyrolysis, derived from the whole POLIMI_BIO1407 mechanism, is constituted by only 44 species reported in Table 3 and is thus suitable for CFD simulations. This skeletal kinetic scheme,

involving 452 elementary and lumped reactions, is reported in the Supplemental Material of this paper, where 4 files are proposed with the following extensions: CKI, NAM, CKT, TRC; indicating respectively the kinetic scheme, the nomenclature, the thermodynamic data and the species transport data.

Table 3: List of species contained in the skeletal mechanism for glycerol pyrolysis studied in this work

N_2	O_2	H	OH	H_2	H_2O	CO	CO_2
HCO	CH_2O	CH_3	CH_2OH	CH_3O	CH_4	CH_3OH	C_2H_2
CH_2CO	$C_2H_2O_2$	C_2H_3	CH_3CO	C_2H_4	CH_3CHO	$C_2H_4O_2$	C_2H_5
C_2H_4OH	C_2H_6	C_2H_5OH	C_2H_3CHO	C_3H_6	C_2H_5CHO	ACETOL	$C_3H_6O_2$
C_3H_8	GLYCEROL	C_4H_4	C_4H_6	SC_4H_7	$CH_2C_3H_5$	CYC_5H_5	CYC_5H_6
C_5H_7	C_6H_6	C_7H_7	C_7H_8				

5 Validation of the model: Comparison with experimental data

As already mentioned, Stein et al. 1983 [32] studied the pyrolysis of glycerol in steam using a tubular, laminar flow quartz reactor. Table 4 reports a comparison between these experimental results and the predicted values obtained with both POLIMI_BIO1407 and the new skeletal mechanism proposed in this work. It is possible to observe that the predictions of the two mechanisms are very similar and in good agreement with experimental data. The kinetic mechanisms are able to characterize the effect of the temperature on the conversion of glycerol and also to predict the yields of the different products. As already discussed by Barker Hemings et al. 2012 [19], and shown in Figure 6, the major species obtained in glycerol pyrolysis are acrolein and acetaldehyde. Moreover, the deviation observed between experimental measurements and model predictions for CO and H_2 could be explained assuming the complete decomposition of formaldehyde, which was not experimentally detected.

Valliyappan et al. 2008 [17] studied the pyrolysis of glycerol at various temperatures (650÷800 °C) and varying flow rates (30÷70 ml/min) in a tubular reactor using different packing materials. The major observed product was syngas with traces of CO_2, CH_4, and C_2H_4. Table 5 shows a comparison between the predictions of the kinetic mechanisms and the measured values. In this case, too, the skeletal scheme provides predictions very close to the ones of the detailed model and in good agreement with the experimental results, especially at low temperatures.

The major deviation for CH_4 and C_2H_4 at 800 °C suggests that their decomposition is not accounted for in the kinetic scheme. Moreover, the increase in the syngas yield also suggests that the steam reforming of methane and ethylene may occur within the reactor. A possible explanation for this discrepancy is supported by a thermodynamic equilibrium calculation, which indicates that at 800 °C the stable products in the system are CO and H_2, whereas methane and other hydrocarbons

should decompose. This reactivity cannot be explained by a gas phase reaction at these temperatures. As already discussed by Barker Hemings et al. [19], experimental evidence of analogous concerted heterogeneous–homogeneous processes are reported in literature Donazzi et al., 2011 [33]. Similar effects were also observed in the study of other oxygenated fuels (ethanol and methyl formate) by Lefkowitz et al. 2012 [34]. A catalytic effect inside the reactor could promote these steam reforming reactions of methane and justify the lack of reactivity:

$$CH_4 + H_2O \rightarrow CO + 3\,H_2 \qquad (1)$$

In a similar way, it is possible to expect some catalytic interactions between ethylene and steam to form oxygenated species, here simply assumed as ethanol.

$$C_2H_4 + H_2O \rightarrow C_2H_5OH \qquad (2)$$

Table 5 also presents the final product distribution obtained by simply including in the skeletal kinetic scheme the two apparent catalytic reactions. Results show a more satisfactory agreement with the experimental data also at high temperatures.

Table 4. Pyrolysis of glycerol in steam at 650, 700 °C and atmospheric pressure. Comparison between the complete kinetic mechanism of Barker-Hemings et al. 2012 [19], the skeletal model of glycerol pyrolysis and the experimental data of Stein et al. 1983 [32].

Temperature		650 °C				700 °C	
	Exp. This work	Predicted Detailed bio1407	Predicted Skeletal mechanism	Exp. Stein et al. [33]	Exp. This work	Predicted Detailed bio1407	Predicted Skeletal mechanism
Glycerol (mole %)	1.69	1.69	1.69	1.04	1.04	1.04	1.04
Conversion (%)	17.6	18	18.2	25	24	23.8	24
Residence time [s]	0.13	0.13	0.13	0.048	0.05	0.05	0.05
Products yield (%)							
CO	30	38	38	58	35	40	40
CO_2	3	4	4	1	2	4	4
Hydrogen	40	29	29	44	39	29	29
Methane	15	9	9	11	15	10	10
Ethylene	12	19	19	17	9	17	17

Figure 7 shows a satisfactory comparison of experimental measurements of Valliyappan et al. 2008 [17] and model simulations in terms of total gas and liquid yields. The carbonaceous residue found

experimentally is probably due to the successive polymerization of tar products that stick to the packing materials within the reactor. Acrolein, for instance, is well known for its polymerization propensity. These phenomena are not included in the gas phase kinetic scheme. These reactions have a negligible effect on the total gas and liquid mass yields but increase significantly the syngas production at high temperature, as already shown in Table 5.

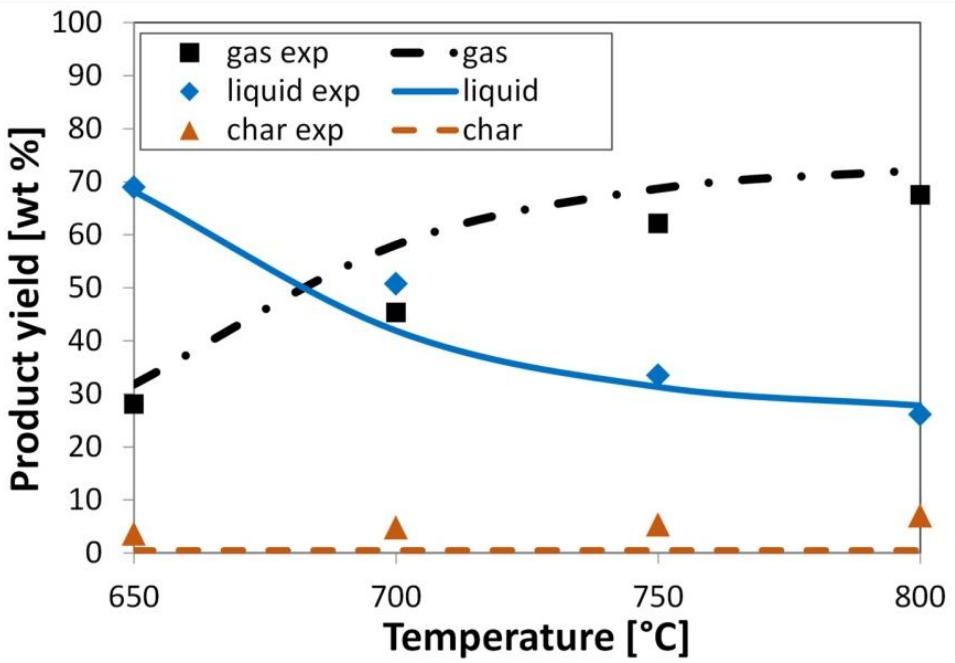

Figure 7: Effect of temperature on product yields during pyrolysis of glycerol at an effective residence time of 1.2 s and 1 atm. Symbols are experimental data taken from Valliyappan et al 2008 [17], model predictions of the skeletal kinetic model are the lines.

Table 5. Effect of temperature on gas product composition during pyrolysis of glycerol at carrier gas flow rate 50 mL/min and atmospheric pressure. Experimental data of Valliyappan et al. 2008 [17]

Temperature	650 °C		800 °C		
Species (dry mol %)	Valliyappan et al. 2008 **[17]**	Skeletal scheme	Valliyappan et al. 2008 **[17]**	Skeletal scheme	Skeletal (including catalytic effect)
H_2	17	19.0	48.6	23.9	37.7
CO	54	46.5	44.9	45.8	45.5
CO_2	0.2	2.6	1	2.5	1.7
CH_4	14.2	16.2	3.3	16.1	8.2
C_2H_4	10.1	11.4	2	9.4	4.8
C_2H_6	2.2	2.4	0.1	0.7	0.6
C_3H_6	2.4	0.	0.1	0.2	0.1
H_2+CO	71	65.5	93.5	69.7	83.1

Kawasaki and Yamane [35] studied the effect of reaction temperature of the pyrolysis of reagent glycerol in N_2 inside a quartz flow reactor at atmospheric pressure. Figure 8 shows a comparison between these experimental measurements and model predictions. Since glycerol is injected as a

liquid, the residence time in the plug flow reactor simulation is assumed to be a fraction (50%) of the nominal residence time reactor to take into account the non ideal behavior of the system. It is possible to observe that the model is able to predict the effect of temperature on the gas conversion efficiency and on the relative yields of the major gas phase species. The gas conversion efficiency is defined by the authors [35] using the measured molar flow rates:

$$\eta_{gas} = \left(\dot{n}_{CO} + \dot{n}_{CO_2} + \dot{n}_{CH_4} + 2\dot{n}_{C_2H_4} + 2\dot{n}_{C_2H_6}\right) \Big/ 3\dot{n}_{Glycerol} \quad (5)$$

The increasing formation of acetylene, C4 species and aromatics explains the reduction of the efficiency moving towards higher temperatures. The formation of gases and syngas, in particular, tends to be overestimated by the model. This deviation is the opposite of the one already discussed in Table 5.

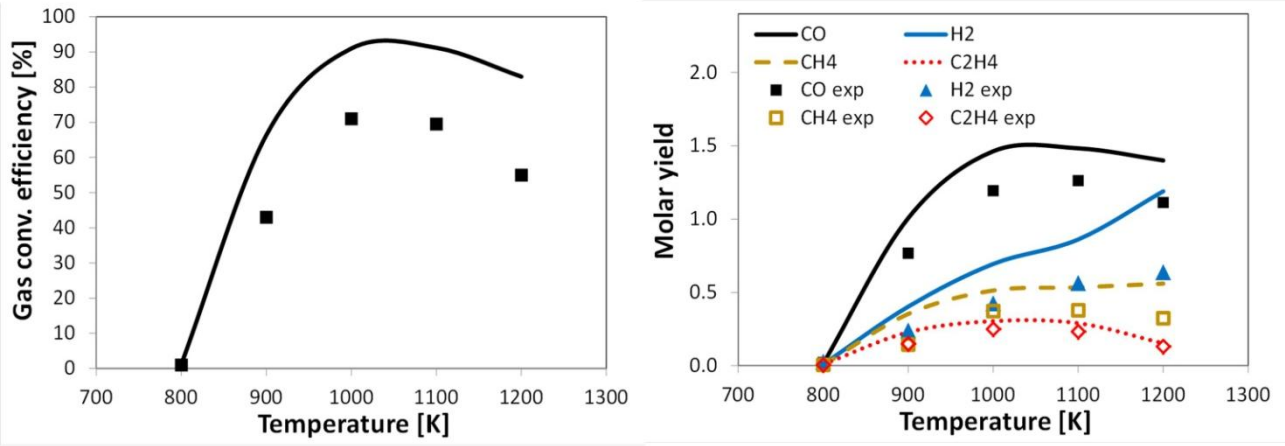

Figure 8: Effect of temperature on gaseous product yields during pyrolysis of glycerol at 1 atm and an effective time equal to half of the nominal residence time in the flow reactor. Symbols are experimental data taken from [35]. Lines represent model predictions of the skeletal kinetic scheme.

6 Discussion

It is important in this discussion section to present the comparison between the performances of glycerol pyrolysis and glycerol steam gasification. In fact, both the processes can be used to produce hydrogen [36-38]. As it can be seen from tables 2,4 and 5 in this paper, hydrogen production through pyrolysis (in a non-catalyzed environment) has acceptable yields only at temperatures above 700°C-800°C. To compare its performance with glycerol two energetic indexes were chosen: the net energy gain and the process efficiency.

The net energy gain is defined in equation 6:

$$NEG = HHVgas * GY - ER \quad (6)$$

Where NEG represents the Net Energy Gain (expressed in kJ/kg glycerol), HHVgas represents the Higher Heating Value of pyrolysis Gas (calculated based on its composition and expressed in kJ/kg), GY represents pyrogas yield (expressed in mass fraction) and ER is the Energy required to promote pyrolysis or gasification processes (expressed in kJ/kg of glycerol). The process efficiency is defined in equation 7:

$$PE = HHVgas * GY / (HHVgl + ER) \quad (7)$$

Where PE represents Process Efficiency (a dimensionless quantity), HHVgas, ER and GY have been already explained, HHVgl is the Higher Heating Value of glycerol (expressed in kJ/kg). The results of the calculation of the two indexes are proposed in table 6.

Table 6: Comparison between the energy performance of pyrolysis and steam gasification of glycerol

Parameter		Pyrolysis at 800°C [17]	Steam gasification at 800°C [17]
Gas conversion		67.3%w	90.60%w
Average Gas Composition	H_2	48.6%v	58.90%v
	CO	44.9%v	30.30%v
	CO_2	1.0%v	4.40%v
	CH_4	3.3%v	4.80%v
Gas Higher Heating Value		18,600 kJ/kg	21,500 MJ/kg
Energy required	Steam	/	3,943 kJ/kg
	Glycerol	5,950 kJ/kg	2,625 kJ/kg
	Total	5,950 kJ/kg	6,568 kJ/mol
Net energy gain (kJ/kg glycerol)		6,568 kJ/kg	12,911 kJ/kg
Ratio between energy in input and energy in output (referred to 1 kilogram of raw material)		0.50	0.76

It can be seen from table 6 that: the net energy gain of the steam gasification process is almost twice that of pyrolysis. Besides the efficiency of the steam gasification process (given by the ratio of the energy in output and the energy in input) is about 0.76 while pyrolysis has an efficiency of 0.50. If the gas will be used in fuel cells this efficiency should be multiplied by the efficiency of the fuel cell itself. These results push for a development of more efficient pyrolysis processes, which can compete with reforming and steam gasification.

An optimized pyrolysis process should:

- introduce a packed bed of biochar to improve volatile yields and their cracking reactions and so hydrogen production;

- in this way, on the one hand, the biochar produced from pyrolysis of biomasses will work as a catalyst;

- on the other hand, it is very probable that using mixtures of glycerol and water as feed material will increase biochar bed porosity by flowing through it.

The possibility to use char as a catalyst to promote volatiles cracking is shown by several works and among them those of prof. Kunio Yoshikawa and coworkers, see [39-42]. New pyrolysis processes are in development, as shown in [43]. Also, water-glycerol mixtures can be a promising material to be used in thermal processes, see [44]. In this way, pyrolysis can become competitive, also compared to the reforming process. Eventually, pyrolysis can be also coupled with steam reforming to improve its performance, see [45]. This is also confirmed by the latest progress on pyroreforming or Thermo-Catalytic Reforming, see [46].

7 Conclusions

Glycerol pyrolysis can be a relevant process to produce hydrogen to be used either as a biofuel for transport purposes or in CHP. Several plants have been proposed to pyrolyze glycerol (fixed beds, pyro-reforming plants etc.) and a zero dimensional model for glycerol pyrolysis has been already developed. In this study, a skeletal kinetic model of glycerol pyrolysis is developed and it allows possible CFD applications for plant optimization and scale up. This is an added value, with respect to the state of the art of pyrolysis modeling, as recently shown by Anca-Couce 2016 [47]. Starting from a detailed kinetic mechanism of more than 4500 reactions involving 137 species, a significant reduction was obtained through the RFA (Reaction Flux Analysis) and the skeletal model simply involves 44 species. The predictions of the skeletal and detailed mechanisms are very similar and in a reasonable agreement with experimental data. The agreement of model predictions improves with the increase of pyrolysis temperature. The new experimental data confirm the increase of non-condensable gases yields, particularly of hydrogen, with the increasing temperatures. Model predictions also confirm that gas yields of 70%w can be achieved at 750-800°C, with hydrogen concentrations up to 44-48%v. These results don't show still an advantage of the pyrolysis process on reforming or steam gasification, because they can achieve yields of gasses above 90%w; so further research will be done on catalytic pyrolysis processes.

Acknowledgements

The laboratories of the Biomass Research Centre and the Fuel Cell Lab of the University of Perugia should be acknowledged for the help in the experimental campaign. The authors would like also to thank Dr. Mathias Mostertz, Head of Clean Energy Technology Biomass Program Linde Innovation Management, for his important information on raw glycerol market and on technical and economic feasibility of glycerol pyroreforming process.

References

[1] Directive 2009/28/EC of the European Parliament and of the Council of 23 April 2009 on the promotion of the use of energy from renewable sources, Official Journal of the European Union http://eur-lex.europa.eu/legal-content/EN/ALL/?uri=CELEX:32009L0028 (accessed 17/09/2016)

[2] USDA Foreign Agriculture Service, Gain Report number: NL4025, EU Biofuels Annual 2014, http://gain.fas.usda.gov/Recent%20GAIN%20Publications/Biofuels%20Annual_The%20Hague_EU-28_7-3-2014.pdf (accessed 7/1/2015)

[3] D'Alessandro B., Bartocci P., Fantozzi F., Gas turbines chp for bioethanol and biodiesel production without waste streams. In: Proceedings of ASME Turbo Expo. vol.1;2011.p.691–700

[4] Fantozzi, F., Bartocci, P., D'Alessandro, B., Arampatzis, S., Manos, B., Public-private partnerships value in bioenergy projects: Economic feasibility analysis based on two case studies, Biomass and Bioenergy, Volume 66, July 2014, Pages 387-397

[5] Manos, B., Partalidou, M., Fantozzi, F., Arampatzis, S., Papadopoulou, O., Agro-energy districts contributing to environmental and social sustainability in rural areas: Evaluation of a local public-private partnership scheme in Greece, Renewable and Sustainable Energy Reviews, Volume 29, 2014a, Pages 85-95

[6] Manos, B., Bartocci, P., Partalidou, M., Fantozzi, F., Arampatzis, S., Review of public-private partnerships in agro-energy districts in Southern Europe: The cases of Greece and Italy, Renewable and Sustainable Energy Reviews Volume 39, November 2014b, Pages 667-678

[7] Authayanun, S., Mamlouk, M., Scott, K., & Arpornwichanop, A.. Comparison of high-temperature and low-temperature polymer electrolyte membrane fuel cell systems with glycerol reforming process for stationary applications. Applied Energy, 2013, 109, 192–201. http://doi.org/10.1016/j.apenergy.2013.04.009

[8] Beatrice, C., Di Blasio, G., Guido, C., Cannilla, C., Bonura, G., & Frusteri, F. (2014). Mixture of glycerol ethers as diesel bio-derivable oxy-fuel: Impact on combustion and emissions of an automotive engine combustion system. Applied Energy, 132, 236–247. http://doi.org/10.1016/j.apenergy.2014.07.006

[9] Beatrice, C., Di Blasio, G., Lazzaro, M., Cannilla, C., Bonura, G., Frusteri, F., Asdrubali, F., Baldinelli, G., Presciutti, A., Fantozzi, F., Bidini, G., Bartocci, P. (2013). Technologies for energetic exploitation of biodiesel chain derived glycerol: Oxy-fuels production by catalytic conversion. Applied Energy, 102, 63–71. http://doi.org/10.1016/j.apenergy.2012.08.006

[10] Martìn, M., & Grossmann, I. E. (2014). Design of an optimal process for enhanced production of bioethanol and biodiesel from algae oil via glycerol fermentation. Applied Energy, 135, 108–114. http://doi.org/10.1016/j.apenergy.2014.08.054

[11] Nanda, M. R., Yuan, Z., Qin, W., Ghaziaskar, H. S., Poirier, M. A., & Xu, C. C. (2014). A new continuous-flow process for catalytic conversion of glycerol to oxygenated fuel additive: Catalyst screening. Applied Energy, 123, 75–81. http://doi.org/10.1016/j.apenergy.2014.02.055

[12] Pedersen, T. H., Grigoras, I. F., Hoffmann, J., Toor, S. S., Daraban, I. M., Jensen, C. U., Rosendahl, L. A. (2016). Continuous hydrothermal co-liquefaction of aspen wood and glycerol with water phase recirculation. Applied Energy, 162, 1034–1041. http://doi.org/10.1016/j.apenergy.2015.10.165

[13] C. Wulf, M. Kaltschmitt, Life cycle assessment of biohydrogen production as a transportation fuel in Germany, Bioresource Technology 150, (2013), 466–475

[14] Encinar J.M., Gonzalez J.F., Martinez G., Sanchez N., Sanguino I. M., Hydrogen production by means pyrolysis and steam gasification of glycerol, International Conference on Renewable Energies and Power Quality, Las Palmas de Gran Canaria (Spain), 13 – 15 Aprile, 2010

[15] Fernandez Y., Arenillas A., Diez M.A., Pis J.J., Menendez J.A., Pyrolysis of glycerol over activated carbons for syngas production, J. Anal. Appl. Pyrolysis 84 (2009) 145–150

[16] Peres A. P. G., de Lima D. R., de Lima da Silva N., Wolf Maciel M. R., Syngas production and optimization from glycerol pyrolysis, International Review of Chemical Engineering - Rapid Communication; 2010, Vol. 2 Issue 2, p305

[17] Valliyappan, T., Hydrogen or Syngas Production from Glycerol Using Pyrolysis and Steam Gasification Processes, A Thesis Submitted to the College of Graduate Studies and Research in partial fulfillment of the requirements for the degree of Master of Science in the Department of Chemical Engineering University of Saskatchewan Saskatoon, Saskatchewan (2004)

476 [18] Valliyappan, T., Bakhshi, N.N., Dalai, A.K., Pyrolysis of glycerol for the production of hydrogen or
477 syngas, Bioresource Technology 99 (2008) 4476–4483

478 [19] Barker-Hemings, E., Cavallotti, C., Cuoci, A., Faravelli, T., Ranzi, E., A detailed kinetic study of
479 pyrolysis and oxidation of glycerol (propane-1,2,3-triol), Combustion Science and Technology, Volume 184,
480 Issue 7-8, 2012, 1164-1178

481 [20] Bidini, G., Fantozzi, F., Bartocci, P., D'Alessandro, B., D'Amico, M., Laranci, P., Scozza, E., Zagaroli,
482 M., Recovery of precious metals from scrap printed circuit boards through pyrolysis, Journal of Analytical
483 and Applied Pyrolysis, 111 (2015), 140–147

484 [21] UNI 14774-2:2010 Solid Biofuels – Determination of Moisture Content – OvenDry Method – Part 2:
485 Total Moisture – Simplified Method. Italian Organizationfor Standardization, Rome, Italy

486 [22] UNI 14775:2010 Solid Biofuels – Determination of Ash Content. Italian Organi-zation for
487 Standardization, Rome, Italy

488 [23] UNI 15104:2011 Solid Biofuels. Determination of Total Content of Carbon,Hydrogen and Nitrogen.
489 Instrumental Methods. Italian Organization for Stan-dardization, Rome, Italy.

490 [24] UNI 14918: Solid Biofuels – Determination of Calorific Value. Italian Organization for Standardization,
491 Rome, Italy.

492 [25] Bartocci, P., Slopiecka, K., Testarmata, F., D'Amico, M., Moriconi, N., Fantozzi, F., Batch pyrolysis
493 reactor: design, realization and preliminary testing on selected biomasses, in: Proceedings of the 20th
494 European Biomass Conference and Exhi-bition, Milan, Italy, 2012

495 [26] Paethanom, A., Bartocci, P., D'Alessandro, B., D'Amico, M., Testarmata, F., Moriconi, N., Slopiecka,
496 K., Yoshikawa, K., Fantozzi, F., A low-cost pyrogas cleaning system for power generation: scaling up from
497 lab to pilot, Appl. Energy 111 (2013), 1080–1088

498 [27] Phuphuakrat, T., Namionka, T., Yoshikawa, K., Tar removal from biomass pyrolysis gas in two-step
499 function of decomposition and adsorption, Applied Energy, 87 (2010), pp.2203-2211

500 [28] Michailos S., Zabaniotou, A., Simulation of Olive Kernel Gasification in a Bubbling Fluidized Bed Pilot
501 Scale Reactor, Journal of Sustainable Bioenergy Systems, 2, (2012), pp. 145-159

502 [29] CEN/TS 15439:2006, Biomass gasification. Tar and particles in product gases. Sampling and analysis

503 [30] Ranzi, E., Frassoldati, A., Grana, R., Cuoci, A., Faravelli, T., Kelley, A.P., Law, C.K., Hierarchical and
504 comparative kinetic modeling of laminar flame speeds of hydrocarbon and oxygenated fuels, Progress in
505 Energy and Combustion Science 38 (2012) 468-501; BIO_1311 mechanism, available at:
506 http://creckmodeling.chem.polimi.it/

507 [31] Stagni, A., Cuoci, A., Frassoldati, A., Faravelli, T., Ranzi, E., A fully coupled, parallel approach for the
508 post-processing of CFD data through reactor network analysis, Computers & Chemical Engineering, Volume
509 60, 10 January 2014, Pages 197–212

510 [32] Stein, Y S., Antal, M J , Jones, M., A study of the gas-phase pyrolysis of glycerol, Journal of Analytical
511 and Applied Pyrolysis, Volume 4, Issue 4, 1983, Pages 283–296

512 [33] Donazzi, A., Livio, D., Maestri, M., Beretta, A., Groppi, G., Tronconi, E., Forzatti, P., Synergy of
513 Homogeneous and Heterogeneous Chemistry Probed by In Situ Spatially Resolved Measurements of

514 Temperature and Composition, Angewandte Chemie International Edition, Volume 50, Issue 17, 2011, pages
515 3943–3946

516 [34] Lefkowitz, J K., Heyne, J S., Won, S H., Dooley, S., Kim, H H., Haas, F M., Jahangirian, S., Dryer, F
517 L., Ju, Y., A chemical kinetic study of tertiary-butanol in a flow reactor and a counterflow diffusion flame,
518 Combustion and Flame 159 (2012) 968–978;

519 [35] Kawasaki, K., Yamane, K., Thermal Decomposition of Waste Glycerol, Proceedings of the
520 International Conference on Power Engineering-09 (ICOPE-09) November 16-20, 2009, Kobe, Japan

521 [36] Authayanun, S., Mamlouk, M., Scott, K., Arpornwichanop, A., Comparison of high-temperature and
522 low-temperature polymer electrolyte membrane fuel cell systems with glycerol reforming process for
523 stationary applications, Applied Energy 109 (2013) 192–201

524 [37] Park, D., Lee, C., Ju Moon, D., Kim, T., Novel macro - micro channel reactor for reforming glycerol
525 produced from biodiesel productions, Energy Procedia 61 (2014) 2075 – 2078

526 [38] Guo, Y., Azmat, M. U., Liu, X., Wang, Y., Lu, G., Effect of support's basic properties on hydrogen
527 production in aqueous-phase reforming of glycerol and correlation between WGS and APR, Applied Energy
528 92 (2012) 218–223

529 [39] Shen, Y., Zhao, P., Shao, Q., Takahashi, F., Yoshikawa, K., In situ catalytic conversion of tar using rice
530 husk char/ash supported nickel–iron catalysts for biomass pyrolytic gasification combined with the mixing-
531 simulation in fluidized-bed gasifier, Applied Energy 160 (2015) 808–819

532 [40] Shen, Y., Chen, M., Sun, T., Jia, J., Catalytic reforming of pyrolysis tar over metallic nickel
533 nanoparticles embedded in pyrochar, Fuel, 159 (2015) 570-579

534 [41] Shen, Y., Wang, J., Ge, X., Chen, M., By-products recycling for syngas cleanup in biomass pyrolysis -
535 An overview, Renewable and Sustainable Energy Reviews, 59 (2016) 1246-1268

536 [42] Shen, Y., Chars as carbonaceous adsorbents/catalysts for tar elimination during biomass pyrolysis or
537 gasification, Renewable and Sustainable Energy Reviews, 43 (2015) 281-295

538 [43] Shirazi, Y., Viamajala, S., Varanasi, S., High-yield production of fuel- and oleochemical-precursors
539 from triacylglycerols in a novel continuous-flow pyrolysis reactor, Applied Energy, 179 (2016) 755–764

540 [44] Setyawan, H. Y., Zhu, M., Zhang, Z., Zhang, D., An Experimental Study of Effect of Water on Ignition
541 and Combustion Characteristics of Single Droplets of Glycerol, Energy Procedia, 75 (2015) 578-583

542 [45] Namioka, T., Saito, A., Inoue, Y., Park, Y., Min, T., Roh, S., Yoshikawa, K., Hydrogen-rich gas
543 production from waste plastics by pyrolysis and low-temperature steam reforming over a ruthenium catalyst,
544 Applied Energy 88 (2011) 2019–2026

545 [46] Neumann, J., Binder, S., Apfelbacher, A., Gasson, J.R., García, P. R., Hornung, A., Production and
546 characterization of a new quality pyrolysis oil, char and syngas from digestate – Introducing the thermo-
547 catalytic reforming process, Journal of Analytical and Applied Pyrolysis 113 (2015) 137–142

548 [47] Anca-Couce, A., Reaction mechanisms and multi-scale modelling of lignocellulosic biomass pyrolysis,
549 Progress in Energy and Combustion Science 53 (2016) 41–79